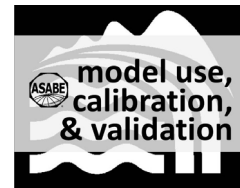


STANMOD: MODEL USE, CALIBRATION, AND VALIDATION

M. Th. van Genuchten, J. Šimůnek, F. J. Leij, N. Toride, M. Šejna



ABSTRACT. This article provides an overview of STANMOD, a Windows-based computer software package for evaluating solute transport in soils and groundwater using analytical solutions of the advection-dispersion equation. The software integrates seven separate codes that have been popularly used over the years for a broad range of one-dimensional and multi-dimensional solute transport applications: the CFITM, CFITIM, CXTFIT, CHAIN, and SCREEN models for one-dimensional transport, and the 3DADE and N3DADE models for multi-dimensional transport. All of the models can be run for direct (forward) problems, and several (CFITM, CFITIM, CXTFIT, and 3DADE) can also be run for inverse problems. CXTFIT further includes a stochastic stream tube model assuming local-scale equilibrium or nonequilibrium transport conditions. The 3DADE and N3DADE models apply to two- and three-dimensional transport during steady unidirectional water flow assuming equilibrium and nonequilibrium transport, respectively. Nonequilibrium transport can be simulated using the assumption of either physical nonequilibrium (two-region or mobile-immobile type transport) or chemical nonequilibrium (two-site partial equilibrium, partial kinetic sorption). The STANMOD software comes with a large number of example applications illustrating the utility of the different codes for a variety of laboratory and field-scale solute transport problems.

Keywords. Analytical solutions, Contaminant transport, Nonequilibrium transport, Parameter estimation, STANMOD.

The solution of many subsurface contaminant transport problems requires the use of appropriate modeling tools consistent with the application. While many field problems require comprehensive numerical models simulating transient water, heat, and/or solute transport (e.g., Šimůnek et al., 2012), some solute transport problems may well be addressed using simplified one-dimensional or multi-dimensional analytical models. As pointed out by Javandel et al. (1984), Leij et al. (1991), Bauer et al. (2001), Vanderborght et al. (2005), Perez-Guerrero et al. (2009), and many others, analytical models are useful for a variety of applications, such as for providing initial or approximate analyses of alternative pollution scenarios, conducting sensitivity analyses to investigate the effects of various parameters or processes on contaminant transport, extrapolating results over large times and spatial scales where numerical solutions become impractical, serving as screening models, estimating transport

parameters from laboratory or well-defined field experiments, providing benchmark solutions for more complex transport processes that cannot be solved analytically, and for validating more comprehensive numerical solutions of the governing transport equations. At the same time, it is also important to recognize the limitations of analytical transport modeling. For example, analytical models are restricted to linear or linearized problems involving homogeneous profiles subject to a uniform unidirectional flow field that is constant in time and space (e.g., no layered profiles or any root water uptake can be considered). In addition, model parameters generally must be constant, while only relatively simple initial and boundary conditions are permitted.

To have flexibility in optimally addressing different transport problems, one may need a toolbox containing a range of computer programs of varying degrees of complexity and dimensionality. Here we describe the Windows-based STANMOD computer software package, which combines a large number of analytical solute transport models that were developed during the past 30 years or more. Most of the models within STANMOD were developed jointly by the U.S. Salinity Laboratory and the University of California, both in Riverside, California, and placed in the public domain (Šimůnek et al., 1999; web-based updates available at www.pc-progress.com/en/Default.aspx?stanmod). The objective of this article is to briefly describe the various codes integrated within STANMOD, which stands for “STudio of ANalytical MODEls,” and to illustrate typical laboratory- and field-scale applications.

Submitted for review in September 2011 as manuscript number SW 9428; approved for publication by the Soil & Water Division of ASABE in May 2012.

The authors are **Martinus Th. van Genuchten**, Professor, Department of Mechanical Engineering, Federal University of Rio de Janeiro, Brazil; **Jiří Šimůnek**, Professor, Department of Environment Sciences, University of California, Riverside, California; **Feike J. Leij**, Professor, Department of Civil Engineering and Construction Engineering Management, California State University, Long Beach, California; **Nobuo Toride**, Professor, Faculty of Bioresources, Mie University, Tsu, Japan; and **Miroslav Šejna**, Director, PC-Progress, Ltd., Prague, Czech Republic. **Corresponding author:** M. Th. van Genuchten, Department of Mechanical Engineering COPPE/LTTC, Federal University of Rio de Janeiro, UFRJ, Rio de Janeiro, RJ, 21945-970, Brazil; phone: +55-21-3264-7025; e-mail: rvan-genuchten@hotmail.com.

Table 1. Overview of computer codes included in the STANMOD software package

Model	Transport Domain	General Description	Initial Condition	Boundary Condition	Parameter Estimation?	Key Reference
CFITM	1D Finite or semi-infinite profile	BTCs only, Equilibrium transport, No production or decay	Constant	Constant or finite pulse	Yes	van Genuchten (1980)
CFITIM	1D Semi-infinite profile	BTCs only, Equilibrium or nonequilibrium transport, No production or decay	Constant	Constant or finite pulse	Yes	van Genuchten (1981a)
CXTFIT	1D Semi-infinite profile	Equilibrium or nonequilibrium transport, Stream tube models, Zero-order production, First-order degradation	Constant, Dirac, exponential, or multiple-step function	Constant, Dirac exponential, or multiple-step functions	Yes	Toride et al. (1999)
CHAIN	1D Semi-infinite profile	Solute decay chains, No production, First-order degradation	Zero initial condition	Constant or finite pulse	No	van Genuchten (1985)
SCREEN	1D Semi-infinite profile	Pesticide screening, First-order degradation, Volatilization	Single-step function versus distance	Volatilization boundary condition	No	Jury et al. (1983)
3DADE	2,3D Semi-infinite Cartesian or cylindrical coordinates	Equilibrium transport, Zero-order production, First-order degradation	Constant, finite parallelepipedal or cylindrical initial condition	Constant or finite pulse	Yes	Leij and Bradford (1994)
N3DADE	2,3D Semi-infinite Cartesian or cylindrical coordinates	Nonequilibrium transport, Zero-order production, First-order degradation	Constant, finite parallelepipedal, or cylindrical initial condition	Constant or finite pulse	No	Leij and Toride (1997)

STANMOD DESCRIPTION

Table 1 gives an overview of the different codes incorporated thus far in STANMOD, along with references for the original codes. The models include the CFITM code for predicting or analyzing measured solute breakthrough data (concentration curves versus time) in terms of the one-dimensional equilibrium advection-dispersion equation (ADE), the CFITIM code for similar problems permitting both physical or chemical nonequilibrium transport, the CXTFIT code allowing predictions and analyses of equilibrium and nonequilibrium transport in time and/or space (including probabilistic analyses of solute transport using stream tube models), the CHAIN code for predicting the transport of solutes subject to consecutive first-order decay chain reactions, the SCREEN code for environmental assessments (transport, degradation, adsorption, and volatilization) of soil-applied organic chemicals, and the 3DADE and N3DADE codes for analyses of multi-dimensional transport problems assuming equilibrium and nonequilibrium conditions, respectively.

All programs within STANMOD are for forward problems in that solute concentrations can be predicted for a prescribed set of transport parameters, such as the pore-water velocity, the dispersion coefficient and, if applicable, zero-order production and first-order degradation coefficients. Several codes (CFITM, CFITIM, CXTFIT, and 3DADE) also permit inverse analyses, in which selected transport parameters can be estimated from observed concentration distributions versus time and/or distance. Parameter estimation in STANMOD is accomplished using a Marquardt-Levenberg type weighted nonlinear least-squares optimization approach (Marquart, 1963) that minimizes the objective function O :

$$O(\mathbf{b}) = \sum_{i=1}^n w_i \left[c_i^*(\mathbf{x}, t) - c_i(\mathbf{x}, t; \mathbf{b}) \right]^2 \quad (1)$$

where n is the number of concentration measurements; $c_i^*(\mathbf{x}, t)$ are observed concentrations at time t and location \mathbf{x} (in one, two, or three dimensions); $c_i(\mathbf{x}, t; \mathbf{b})$ represent corresponding model predictions for the vector \mathbf{b} of unknown transport parameters; and w_i are weights associated with a particular concentration data point.

The Marquardt-Levenberg parameter estimation approach as implemented in the STANMOD codes assumes that the variance-covariance (weighting) matrices, which provide information about the measurement accuracy, are diagonal (Šimůnek and Hopmans, 2002). The method uses a local optimization gradient procedure that requires initial estimates of the parameters to be optimized. The behavior of objective function O in the neighborhood of this initial estimate is used to select a direction vector, from which updated values of the unknown parameter vector \mathbf{b} in equation 1 are determined. Depending upon the problem being considered (i.e., the magnitude of the measurement errors and the number of parameters being optimized), the objective function may sometimes lack a well-defined global minimum, or may have several local minima in parameter space. The optimization may then become sensitive to the initial values of the optimized parameters. Depending on the initial estimate, the final solution of the calibration in such cases may then not be the global minimum but instead a local minimum. Consequently, we generally recommend repeating the minimization problem with different initial estimates of the optimized parameters, and then selecting those parameter values among the different runs that pro-

vide the lowest value of the objective function $O(\mathbf{b})$. Generally, however, the parameter estimation approach in STANMOD has proven to be very robust for most transport problems, unless a large number of parameters are determined simultaneously (e.g., for nonequilibrium transport) from data that are noisy or that are not providing good resolution of the expected concentration distribution, or when the inverse solution shows strong correlation between some of the estimated parameters (such as sometimes is the case between the pore-water velocity and the retardation factor).

Not further discussed in this article is the general issue of model validation as applied to analytical solutions. Many references are provided showing a wide range of applications of the various codes within STANMOD, including comparisons with observed data versus distance and/or time. Still, as mentioned earlier, the codes in most cases are restricted to very specific situations, such as homogeneous soils and constant fluid flow regimes typical of analytical solutions. Validation of simplified or approximate models is inherently problematic in that results cannot be extrapolated to more general transient flow conditions generally encountered in the field. We also refer to discussions by Konikow and Bredehoeft (1992) and Oreskes et al. (1994), among many others later, about the presumed difficulties of model validation in general. Still, we note that the mathematical accuracy of all solutions and codes within STANMOD has been tested thoroughly ("mathematically verified") through comparisons with other codes, against numerical software such as the HYDRUS codes (Šimůnek et al., 2012), or otherwise as documented in the various manuals.

We next briefly describe the different analytical solute transport models included in STANMOD and discuss some typical examples, most of which are installed with the software. The software itself can be downloaded freely from the STANMOD homepage (www.pc-progress.com/en/Default.aspx?stanmod). Detailed descriptions of most or all models are given in the original manuals, which can be downloaded from several websites, including the STANMOD site. The manuals provide complete descriptions of the governing transport equations, applicable initial and boundary conditions, the derived analytical solutions, listings of the older FORTRAN programs, as well as detailed descriptions of illustrative examples. The graphics-based user-interface of STANMOD is for MS Windows environments and is mostly based on libraries developed for the HYDRUS-1D and HYDRUS (2D/3D) software packages (Šimůnek et al., 2008a, 2008b; Šejna et al., 2011). All computational programs within STANMOD were written in FORTRAN (essentially identical to the original codes) and the graphical user interfaces in MS Visual C++.

THE CFITM CODE

The CFITM code (van Genuchten, 1980) may be used to analyze observed solute concentration distributions versus time using analytical solutions of the one-dimensional equilibrium advection-dispersion equation given by:

$$R \frac{\partial c}{\partial t} = D \frac{\partial^2 c}{\partial x^2} - v \frac{\partial c}{\partial x} \quad (2)$$

where c is the solution concentration, x is distance, t is time, D is the dispersion coefficient, v is the average pore water velocity (water flux q divided by the water content Θ), and R is the retardation factor, defined as:

$$R = 1 + \frac{\rho k}{\theta} \quad (3)$$

where ρ is the dry soil bulk density, and k (sometimes denoted as K_d) is a linear partitioning or distribution coefficient of the solute between the liquid and solid phases.

The CFITM code assumes the use of dimensionless parameters, in which the initial and input (boundary) concentrations are scaled to zero and one, respectively. Initial applications of the code focused on the analyses of the observed effluent curves from finite laboratory columns of length L . Introduction of the column Peclet number, P , given by:

$$P = \frac{vL}{D} \quad (4)$$

leads then to the dimensionless ADE as follows:

$$R \frac{\partial c}{\partial T} = \frac{1}{P} \frac{\partial^2 c}{\partial X^2} - \frac{\partial c}{\partial X} \quad (5)$$

where dimensionless time T (often referred to as pore volume) and distance X are given by:

$$T = \frac{vL}{L} \quad (6a)$$

$$X = \frac{x}{L} \quad (6b)$$

and c is the normalized concentration, in contrast with equation 2.

CFITM provides analytical solutions of equation 5 subject to both first-type (Dirichlet or concentration type) and third-type (Cauchy or flux type) boundary conditions at the inlet ($x = 0$), and either a zero concentration gradient at the outlet of the finite column ($0 \leq x \leq L$) or assuming that the finite column is part of a semi-infinite system ($0 \leq x < \infty$). The concentration at the outlet is then assumed not to be affected by the exit boundary. As shown elsewhere (e.g., van Genuchten and Parker, 1984; Skaggs and Leij, 2002), the proper mass-conservative analytical solution to use is the classical solution of Lapidus and Amundson (1952) for the flux-averaged concentration leaving the column at $x = L$:

$$c(X, T) \equiv A(X, T) = \frac{1}{2} erfc \left[\frac{\sqrt{P}(RX - T)}{2\sqrt{RT}} \right] + \frac{1}{2} e^{PX} erfc \left[\frac{\sqrt{P}(RX - T)}{2\sqrt{RT}} \right] \quad (7)$$

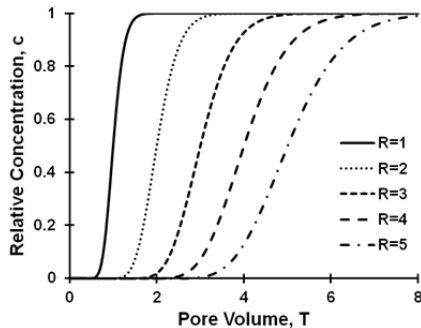


Figure 1. Calculated breakthrough curves for different values of the retardation factor ($R = 1, 2, 3, 4$, and 5) assuming $P = 50$.

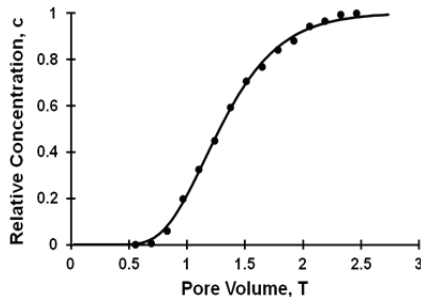


Figure 2. Observed (circles) and fitted (solid line) breakthrough curves for Cr^{6+} transport through a 5 cm long soil column ($P = 18.6$, $R = 1.348$). Unpublished data from Wierenga (1980).

where erfc is the complementary error function.

Here we give two example applications using CFITM. Figure 1 is for a relatively simple forward problem in which solute breakthrough curves (BTCs) are calculated using equation 7 for different values of the retardation factor (R) and assuming a value of 50 for the Peclet number (P).

Figure 2 is for an inverse problem in which equation 7 is fitted to observed Cr^{6+} data (Wierenga, 1980, unpublished data; van Genuchten, 1980). This is actually one of the CFITM examples (EXAMPLE2) installed with STANMOD. The analytical solution in this case was for a finite medium assuming a third-type input boundary condition and a zero concentration gradient at the exit boundary (solution not further given here), in which case the resident and flux concentrations at the outlet become identical (van Genuchten and Parker, 1984). The example illustrates the convenient way in which transport parameters can be determined from concentration distributions by fitting analytical solutions to the observed data. The unknown parameters in this case were the column Peclet number (P) and the retardation factor (R) but could also include as needed the dimensionless pulse time ($T_o = vt_o/L$) when a finite solute pulse of duration t_o is applied, rather than a single-step input function. The solution for the flux concentration leaving the column is then given by:

$$c(X, T) = \begin{cases} A(X, T) & 0 < t \leq t_o \\ A(X, T) - A(X, T - T_o) & t > t_o \end{cases} \quad (8)$$

where $A(x,t)$ is the solution for the constant inlet concentration (van Genuchten, 1980).

THE CFITIM CODE

The CFITIM code (van Genuchten, 1981a) is similar to CFITM but extended to analytical solutions for physical or chemical nonequilibrium transport problems. As opposed to CFITM, however, CFITIM only considers solutions for semi-infinite media. Physical nonequilibrium refers to situations in which physical phenomena such as the presence of immobile water pockets in the medium (e.g., as in aggregated soils or fractured rock) are responsible for the nonequilibrium situation. The governing equations in this case are (van Genuchten and Wierenga, 1976):

$$(\theta_m + f\varphi k) \frac{\partial c_m}{\partial t} = \theta_m D_m \frac{\partial^2 c_m}{\partial x^2} - \theta_m v_m \frac{\partial c_m}{\partial x} - \alpha(c_m - c_{im}) \quad (9a)$$

$$[\theta_{im} + (1-f)\varphi k] \frac{\partial c_{im}}{\partial t} = \alpha(c_m - c_{im}) \quad (9b)$$

where the subscripts m and im refer to the mobile and immobile regions of the soil, f is the fraction of sorption sites located in the mobile region, α is a first-order mass transfer coefficient, and v_m is the pore-water velocity for the mobile phase (q/θ_m). Models based on equations 9a and 9b are alternatively referred to as mobile-immobile transport models, dual-porosity transport models, or two-region models.

Similar to equation 5, equations 9a and 9b can be put in dimensionless form as follows:

$$\beta R \frac{\partial c_m}{\partial T} = \frac{1}{P_m} \frac{\partial^2 c_m}{\partial X^2} - \frac{\partial c_m}{\partial X} - \omega(c_m - c_{im}) \quad (10a)$$

$$(1-\beta)R \frac{\partial c_{im}}{\partial t} = \omega(c_m - c_{im}) \quad (10b)$$

where R is the same as before, and additionally:

$$P_m = \frac{v_m L}{D} \quad (11a)$$

$$\beta = \frac{\theta_m + f\varphi k}{\theta R} \quad (11b)$$

$$\omega = \frac{\alpha L}{q} \quad (11c)$$

The analytical solution of equations 10a and 10b, again in terms of the flux-averaged concentration applicable to column effluent curves, is given by equation 8 with $A(x,t)$ now defined as (Skaggs and Leij, 2002, among others):

$$c(X, T) = \int_0^T \frac{X}{\tau} \sqrt{\frac{\beta P_m R}{4\pi\tau}} \exp\left[-\frac{P_m(\beta RX - \tau)}{4\beta R\tau}\right] \times [1 - J(b, a)] d\tau \quad (12)$$

where $J(b,a)$ is Goldstein's J function, and:

$$a = \frac{\omega\tau}{\beta R} \quad (13a)$$

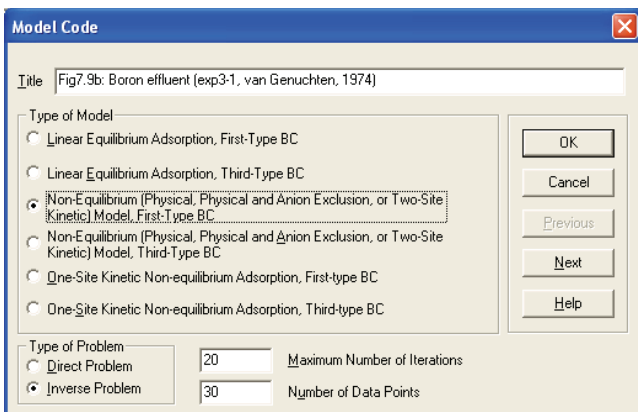


Figure 3. CFITIM window for selecting one of three possible transport models, the desired inlet boundary condition (BC), the type of problem being considered (direct or inverse), the maximum number of iterations for the iterative inverse solution, and the number of data points to be fitted.

$$b = \frac{\omega(T - \tau)}{(1-\beta)R} \quad (13b)$$

Mathematically, very similar equations can also be formulated for chemical nonequilibrium based on the assumption that adsorption does not proceed at an equal rate for all sorption sites on the solid phase. The one-site and two-site nonequilibrium transport equations are examples of this approach. The dimensionless equations are then exactly the same as given by equation 10 (van Genuchten and Wierenga, 1976) but with a different definition of the dimensionless parameter β .

The dimensionless transport model given by equations 10a and 10b contains four dimensionless parameters that can be fitted to observed data: the column Pelet number (P_m), the retardation factor (R), a dimensionless nonequilibrium partitioning coefficient (β) having values between 0 (all nonequilibrium) and 1 (all equilibrium), and a dimensionless mass transfer coefficient (ω). Additionally, again, the dimensionless pulse time (T_o) could be fitted to the data if the amount of solute mass entering the column must also be estimated. Refer to the manual (van Genuchten, 1981a) for a detailed discussion of the governing equations.

Here we show an example CFITIM application, based on figure 7.9b of van Genuchten (1981a), but with a first-type input boundary condition appropriate for flux-averaged concentrations typical of column effluent curves. In this case, the dimensionless nonequilibrium transport model was fitted to observed boron effluent data from a 30 cm long soil column (van Genuchten, 1974). Figure 3 shows the CFITIM window where the current project and its boundary conditions are defined, including the option of running an inverse problem (lower left corner of fig. 3), the maximum number of permitted iterations in the inverse problem (20 in this case), and the number of data points that are fitted (30 in this example). Figure 4 shows the results of this application, including values of the fitted parameters.

THE CXTFIT CODE

To our knowledge, CFITM and CFITIM were the first

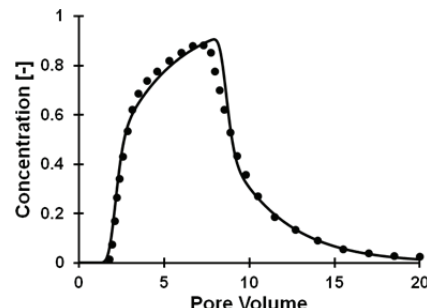


Figure 4. Observed (circles) and fitted (solid line) breakthrough curves for boron transport through a 30 cm long soil column filled with Glendale clay loam (van Genuchten, 1974). The project involved fitting five dimensionless parameters of the physical nonequilibrium model to 30 data points ($P = 37.9$, $R = 3.89$, $\beta = 0.625$, $\omega = 0.650$, and $T_o = 6.187$).

computerized parameter estimation codes that considered inverse analyses of laboratory soil column breakthrough data in terms of equilibrium and nonequilibrium transport models. The models were updated later in very significant ways, first by Parker and van Genuchten (1984) and subsequently by Toride et al. (1999), to produce the widely used CXTFIT code. CXTFIT allows analyses of concentration distributions versus time as well as versus depth (both forward and inverse problems), permits the use of the standard equilibrium and nonequilibrium transport formulations, and includes a variety of stochastic stream tube models that consider the effects of areal variations in the pore-water velocity on field-scale transport. The code can be applied to a broad range of laboratory and field data due to the implementation of very flexible initial and boundary conditions, the inclusion of general zero-order production and first-order degradation processes, and by considering both equilibrium and nonequilibrium transport in the stochastic stream tube models.

Examples included in the CXTFIT code are divided into three separate groups (workspaces). The first group (Direct) contains direct problems, the second group (Inverse) involves inverse problems, and the third group (Stochast) contains stochastic stream tube applications. Most examples were taken from the most recent CXTFIT manual (Toride et al., 1999), and book chapters by van Genuchten and Cleary (1979) and Leij and Toride (1998). Here we give one example for each of the three workspaces. Hundreds of other examples can be retrieved readily from the peer-reviewed literature, with applications involving the transport of broad range of chemicals, including nonadsorbing tracers, pesticides, heavy metals, radionuclides, and other organic and inorganic chemicals. We list here rather arbitrarily a few publications in which the CXTFIT codes have been used successfully to estimate transport parameters from observed concentration distributions versus time and/or distance: Gamarlinger et al. (1990), Jacobsen et al. (1992a, 1992b), Pivetz and Steenhuis (1995), Spurlock et al. (1995), Huang et al. (1995), Jensen et al. (1996), Seuntjens et al. (2001), Kay and Conklin (2001), Kamra et al. (2001), Antoniadis and McKinley (2003), Pace et al. (2003), Gaur et al. (2003), Tilahun et al. (2005), Duke et al. (2007), Wellman et al. (2008), Mayer et al. (2008), Srivastava et al. (2009), Tao et al. (2009), Köhne et al. (2011),

and Koestel et al. (2011). Similar applications can be found for the older CFITM and CFITIM codes but are not further listed here.

DIRECT CXTFIT APPLICATION

The CXTFIT code comes with many preprogrammed forward problems, such as showing the effects of various parameters, including of productions and decay, on distributions versus distance or time. Here we consider a direct problem showing the effect of first-order degradation on concentration distributions versus distance. The governing transport equation for this case is given by:

$$R \frac{\partial c}{\partial t} = D \frac{\partial^2 c}{\partial x^2} - v \frac{\partial c}{\partial x} - \mu c + \gamma \quad (14)$$

where μ is a first-order degradation rate constant, and γ is a zero-order production term. Assuming a pulse type solute application with concentration C_o to a profile having an initial concentration C_i , the analytical solution for the volume-averaged (resident) concentration is given by (van Genuchten and Alves, 1982; Toride et al., 1999):

$$c(x, t) = \begin{cases} C_o B(x, t) + C_i A(x, t) \\ + \frac{\gamma}{\mu} [1 - A(x, t) - B(x, t)] & 0 < t \leq t_o \\ C_o [B(x, t) - B(x, t - t_o)] + C_i A(x, t) \\ + \frac{\gamma}{\mu} [(1 - A(x, t) - B(x, t))] & t > t_o \end{cases} \quad (15)$$

where

$$A(x, t) = \exp\left(-\frac{\mu t}{R}\right) \left\{ 1 - \frac{1}{2} \operatorname{erfc}\left[\frac{Rx - vt}{2\sqrt{DRt}}\right] \right. \\ \left. - \sqrt{\frac{v^2 t}{\pi DR}} \exp\left[-\frac{(Rx - vt)^2}{4DRt}\right] \right. \\ \left. + \frac{1}{2} \left(1 + \frac{vx}{D} + \frac{v^2 t}{DR}\right) \exp\left(\frac{vx}{D}\right) \operatorname{erfc}\left[\frac{Rx + vt}{2\sqrt{DRt}}\right] \right\} \quad (16)$$

$$B(x, t) = \frac{v}{u+v} \exp\left[\frac{(v-u)x}{2D}\right] \operatorname{erfc}\left[\frac{Rx - ut}{2\sqrt{DRt}}\right] \\ - \frac{v}{u-v} \exp\left[\frac{(v+u)x}{2D}\right] \operatorname{erfc}\left[\frac{Rx + ut}{2\sqrt{DRt}}\right] \\ + \frac{v^2}{2\mu D} \exp\left(\frac{vx}{D} - \frac{\mu t}{R}\right) \operatorname{erfc}\left[\frac{Rx + vt}{2\sqrt{DRt}}\right] \quad (17)$$

$$u = \sqrt{v^2 + 4\mu D} \quad (18)$$

Equation 15 holds for nonzero values of the first-order degradation coefficient (μ). When $\mu = 0$, the solution reduces to (van Genuchten and Alves, 1982):

$$c(x, t) = \begin{cases} C_o A(x, t) + C_i [1 - A(x, t)] \\ + \frac{\gamma}{R} B(x, t) & 0 < t \leq t_o \\ C_o [A(x, t) - A(x, t - t_o)] \\ + C_i [1 - A(x, t)] + \frac{\gamma}{R} B(x, t) & t > t_o \end{cases} \quad (19)$$

where

$$A(x, t) = \frac{1}{2} \operatorname{erfc}\left[\frac{Rx - vt}{2\sqrt{DRt}}\right] \\ + \sqrt{\frac{v^2 t}{\pi DR}} \exp\left[-\frac{(Rx - vt)^2}{4DRt}\right] \\ - \frac{1}{2} \left(1 + \frac{vx}{D} + \frac{v^2 t}{DR}\right) \exp\left(\frac{vx}{D}\right) \operatorname{erfc}\left[\frac{Rx + vt}{2\sqrt{DRt}}\right] \quad (20)$$

$$B(x, t) = t + \left(\frac{Rx - vt + \frac{DR}{v}}{2v} \right) \operatorname{erfc}\left[\frac{Rx - vt}{2\sqrt{DRt}}\right] \\ - \sqrt{\frac{t}{4\pi DR}} \left(Rx + vt + \frac{2DR}{v} \right) \exp\left[-\frac{(Rx - vt)^2}{4DRt}\right] \\ + \left[\frac{t}{2} - \frac{DR}{2v^2} + \frac{(Rx + vt)^2}{4DR} \right] \exp\left(\frac{vx}{D}\right) \operatorname{erfc}\left[\frac{Rx + vt}{2\sqrt{DRt}}\right] \quad (21)$$

The above solutions are given in a structure that reflects the derivation of the analytical solutions using superposition principles (Toride et al., 1999) as well as entry of the model input parameters into CXTFIT using its graphical interface. They consist of the sum of solutions for a boundary value problem (the terms containing the input concentration C_o in eqs. 15 and 19), an initial value problem (the terms containing the initial condition C_i), and a production value problem (the terms containing the zero-order production coefficient γ).

Figure 5 shows results for one example of a forward problem with CXTFIT (FIG71 of the Direct workspace). Calculated resident concentrations are presented versus distance 7.5 days after starting the application of a 5-day solute pulse ($t_o = 5$ d) with a concentration $C_o = 1 \text{ mg L}^{-3}$ to an initially solute-free medium ($C_i = 0$) and assuming degradation

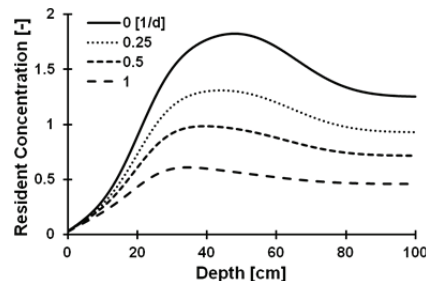


Figure 5. Calculated concentration distributions versus depth showing the effect of degradation. The degradation coefficient increased from $\mu = 0$ (top curve) to $\mu = 1 \text{ d}^{-1}$ (bottom curve).

coefficients (μ) of 0, 0.25, 0.5, and 1 d^{-1} . Other parameters for this example are $v = 25 \text{ cm d}^{-1}$, $D = 35.5 \text{ cm}^2 \text{ d}^{-1}$, $R = 3$ and $\gamma = 0.5 \text{ mg L}^{-3} \text{ d}^{-1}$. As expected, results indicate decreasing concentrations as the degradation coefficient increases.

INVERSE CXTFIT APPLICATION

In this example, the pore-water velocity (v) and dispersion coefficient (D) are estimated from observed concentrations at three different depths (11, 17, and 23 cm) measured with four-electrode conductivity sensors (Shiozawa, 1988, unpublished data). The experiments involved the continuous application of a 0.01 M NaCl solution to an initially solute-free saturated sand ($\theta = 0.30$), followed by leaching with solute-free water during unsaturated conditions ($\theta = 0.12$). The analytical solution for the resident concentration in this case is given by equations 19 through 21 with $\gamma = 0$ (Lindstrom et al., 1967). Results for this example (projects FIG73A and FIG73B of the Inverse workspace of CXTFIT) are shown in figure 6, along with the fitted parameter values for v and D (R was assumed to be unity). Fitting all three curves simultaneously (either the breakthrough curves or the leaching curves) with CXTFIT yielded about the same results as fitting v and D separately for each curve at the three depths. However, the dispersivity (D/v) for the unsaturated sand was found to be about 3 times larger than the dispersivity for the saturated experiment (Toride et al., 1999, 2003).

STOCHASTIC CXTFIT APPLICATION

CXTFIT also contains several examples demonstrating the use of stochastic stream tube models (Toride et al., 1999). The modeling approach assumes that a field may be viewed as a collection of independent vertical soil columns, often referred to as "stream tubes" (Dagan, 1993; Toride and Leij, 1996a; Vanderborght et al., 2006). Local-scale

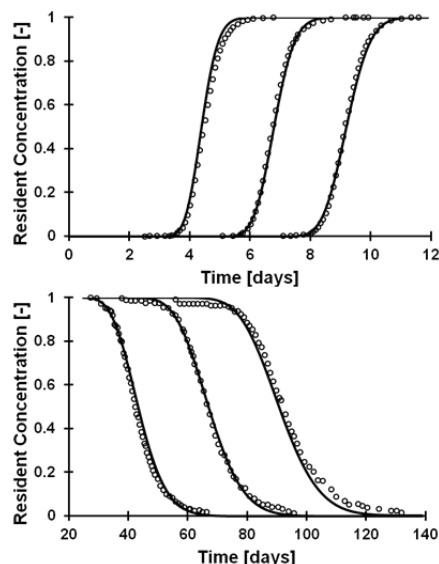


Figure 6. Observed (open circles) and fitted (solid lines) breakthrough curves for transport into a saturated sand (top) or leaching from unsaturated sand (bottom). In this example the three breakthrough curves, measured at $x = 11, 17$, and 23 cm inside the column, were fitted simultaneously (yielding $v = 2.50 \text{ cm min}^{-1}$ and $D = 0.130 \text{ cm}^2 \text{ min}^{-1}$), as were the three leaching curves ($v = 0.253 \text{ cm min}^{-1}$ and $D = 0.0391 \text{ cm}^2 \text{ min}^{-1}$).

transport in each stream tube can be described deterministically using one of several transport models. In CXTFIT, these are the traditional equilibrium and nonequilibrium transport models, as discussed earlier. Transport at the field scale is then modeled by assuming that selected parameters in these transport models for each tube are the realization of a stochastic process, with the mean solute concentration of the entire field given by the ensemble average of the local concentrations of all stream tubes. Stochastic variables in the CXTFIT stream tube models are the pore-water velocity (v) in combination with either the dispersion coefficient (D), the partitioning coefficient for linear sorption (k), or the first-order rate coefficient for nonequilibrium adsorption (α). The three different pairs of random variables are described using bivariate lognormal joint probability density functions denoted as $f(v,D)$, $f(v,k)$, and $f(v,\alpha)$ (Toride and Leij, 1996a, 1996b). Two additional stochastic parameters can be included, provided they are perfectly correlated with v .

We show here one forward and one inverse problem. The forward problem demonstrates the effect of correlation ($\rho_{vk} = -1, 0, +1$) between the pore water velocity (v) and the distribution coefficient (k) on calculated field-scale resident concentration (c_r) profiles (project FIG713 of the Stochast workspace; figure 7.13 of Toride et al., 1999). Field-scale concentrations at $t = 5 \text{ d}$ resulting from a Dirac delta input at $t = 0$ were calculated versus depth for perfect negative correlation, no correlation, and perfect positive correlation between v and k . Values of the other parameters in this example were $\langle v \rangle = 50 \text{ cm d}^{-1}$, $\sigma_v = 0.2$, $D = 20 \text{ cm}^2 \text{ d}^{-1}$, $\langle k \rangle = 1 \text{ g}^{-1} \text{ cm}^3$, $\sigma_k = 0.2$, $\langle R \rangle = 5$, and $\rho_b/\theta = 4 \text{ g cm}^{-3}$, where $\langle \rangle$ indicates an ensemble average, σ_v is the standard deviation of the log transform of v , and σ_k is the standard deviation of the log transform of k . Results, shown in figure 7, indicate that negative correlation between v and k (which implies that v and R are inversely correlated) leads to increased spreading in the field-scale concentrations. More details of this example are given by Toride and Leij (1996a) and Toride et al. (1999).

The stochastic option of CXTFIT, together with parameter estimation, is demonstrated with the FIG712 project of the Inverse workspace. The example (figure 7.12 of Toride et al., 1999) concerns the analyses of observed resident concentrations in a 0.64 ha field to which a bromide pulse was applied for 1.69 d, followed by leaching with solute-free water (Jury et al., 1982). The stream tube model was used to estimate the mean pore-water velocity $\langle v \rangle$, the

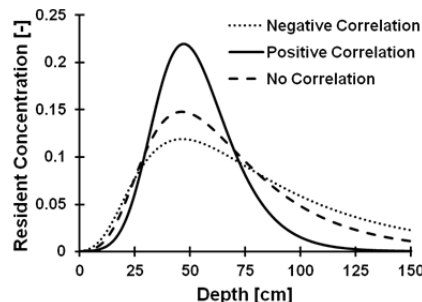


Figure 7. Effect of perfect positive and negative correlations and no correlation between v and k on field-scale resident concentration profiles. Negative correlation caused the most spreading.

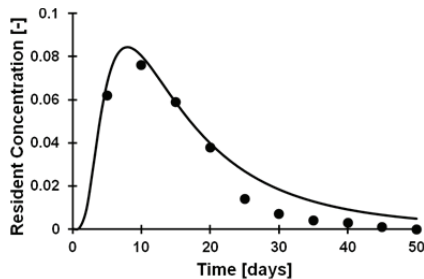


Figure 8. Observed (circles) and fitted values (solid line) of the resident concentration for field-scale bromide transport (after Toride et al., 1999).

mean dispersion coefficient $\langle D \rangle$, and the standard deviation (σ_v) of the log transform of v from areally averaged concentrations at a depth of 30 cm. The approach assumed perfect positive correlation between v and D such that $\rho_{vD} = +1$ and $\sigma_v = \sigma_D$, which implies that the local-scale dispersivity, λ ($= D/v$), is the same for all stream tubes (Toride and Leij, 1996a). Results are shown in figure 8. Solution of the inverse problem yielded $\langle v \rangle = 30.5 \text{ mm d}^{-1}$, $\sigma_v = \sigma_D = 0.8$, and $\langle D \rangle = 2.5 \text{ mm}^2 \text{ d}^{-1}$. The example shows that local-scale dispersion will have a relatively minor effect on field-scale transport when the stream tube model is used.

THE CHAIN CODE

The CHAIN code (van Genuchten, 1985) may be used to analyze the advective-dispersive transport of solutes subject to sequential first-order decay reactions. Examples are the subsurface transport of various interacting nitrogen species, pesticides, chlorinated hydrocarbons, radionuclides, pharmaceuticals, and explosives. The CHAIN code considers the transport of up to four species involved in these types of decay chains. The governing transport equations for such a system are given by:

$$R_1 \frac{\partial c_1}{\partial t} = D \frac{\partial^2 c_1}{\partial x^2} - v \frac{\partial c_1}{\partial x} - \mu_1 c_1 \quad (22a)$$

$$R_i \frac{\partial c_i}{\partial t} = D \frac{\partial^2 c_i}{\partial x^2} - v \frac{\partial c_i}{\partial x} + \mu_{i-1} c_{i-1} - \mu_i c_i \quad (i = 2, 4) \quad (22b)$$

where the subscript i refers to the i th member of the decay chain. Like equation 14, equations 22a and 22b hold for situations where degradation occurs only in the liquid phase. When radionuclides are considered, decay occurs equally in the liquid and adsorbed phases, which means that retardation factors must be added to the first-order terms, i.e., each μ_i in equations 22a and 22b must be replaced by $\mu_i R_i$ (van Genuchten, 1981b, 1985). This option is directly available in CHAIN. For situations with unequal degradation rates in the liquid and solid phases, the value of each μ_i must be adjusted and defined by the user upon input.

The analytical solutions in CHAIN hold for very general first- and third-type inlet boundary conditions and a solute-free initial semi-infinite soil profile. For a third-type inlet condition applicable to resident concentrations, the bounda-

ry condition is of the form:

$$\left(-D \frac{\partial c}{\partial x} + vc \right)_{x=0} = \begin{cases} vf_i(t) & 0 < t \leq t_o \\ 0 & t > t_o \end{cases} \quad (23)$$

where

$$\begin{aligned} f_1(t) &= B_1 e^{-\lambda_1 t} \\ f_2(t) &= B_2 e^{-\lambda_1 t} + B_3 e^{-\lambda_2 t} \\ f_3(t) &= B_4 e^{-\lambda_1 t} + B_5 e^{-\lambda_2 t} + B_6 e^{-\lambda_3 t} \\ f_4(t) &= B_7 e^{-\lambda_1 t} + B_8 e^{-\lambda_2 t} + B_9 e^{-\lambda_3 t} + B_{10} e^{-\lambda_4 t} \end{aligned} \quad (24)$$

in which the coefficients λ_i ($i = 1, 4$) and B_i ($i = 1, 10$) are all constants. The multiple terms of equation 24 are a consequence of decay reactions within the waste site itself (e.g., an industrial waste site, landfill, or nuclear waste repository), and the slow release of the solutes from the waste into the soil profile (van Genuchten, 1985).

Many scenarios can be accounted for with the above boundary conditions. For one particular release process, the constants B_j are related to each other through the Bateman equations (Bateman, 1910; Higashi and Pigford, 1980). Refer to the article by van Genuchten (1985) for a detailed discussion of the decay chain boundary conditions, as well as the resulting analytical solutions. Because of their complexity, these solutions are not repeated here. Here we provide only one relatively simple example involving the three-species nitrification chain $\text{NH}_4^+ \rightarrow \text{NO}_2^- \rightarrow \text{NO}_3^-$ (project NITROG in the CHAIN workspace of STANMOD). Results are shown in figure 9 for the following parameter values: $v = 1 \text{ cm h}^{-1}$, $D = 0.18 \text{ cm}^2 \text{ h}^{-1}$, $t = 100 \text{ d}$, $R_1 = 2$, $R_2 = R_3 = 1$, $\mu_1 = 0.01 \text{ h}^{-1}$, $\mu_2 = 0.1 \text{ h}^{-1}$, $\mu_3 = 0$, $B_1 = 1$, $B_i = 0$ ($i = 2$ through 10), $\lambda_i = 0$ ($i = 1$ through 4), and $t = 200 \text{ h}$.

The above example is a classic application of consecutive decay chains, first published by Cho (1971). A few other studies in which the CHAIN model within STANMOD, or some of its predecessors, have been used for various solutes and applications are described by Wernberg (1998), Pontedero et al. (2007), Srinivasan and Clement (2008), Perez-Guerrero et al. (2009, 2010), and Kasteel et al. (2010).

THE SCREEN CODE

The SCREEN code is based on a behavior assessment

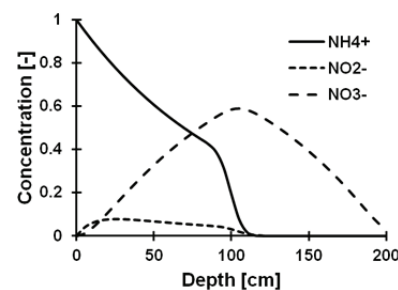


Figure 9. Calculated concentration distributions versus depth of the nitrogen nitrification decay chain $\text{NH}_4^+ \rightarrow \text{NO}_2^- \rightarrow \text{NO}_3^-$ (after Cho, 1971; van Genuchten, 1985).

model developed by Jury et al. (1983) to describe the fate and transport of soil-applied organic chemicals. The model assumes linear, equilibrium partitioning between the liquid, solid, and gaseous phases, first-order degradation, and chemical losses to the atmosphere by volatilization through a stagnant air boundary layer above the soil surface. The model is intended to classify and screen organic chemicals for their relative susceptibility to different loss pathways (volatilization, leaching, and degradation) in soil and air. SCREEN requires knowledge of the organic carbon partition coefficient (K_{oc}), Henry's constant (K_H), and a net first-order degradation rate coefficient (μ) or the chemical half-life.

Jury et al. (1983) formulated their transport equations in terms of the total concentration c_T ($= \theta R_T C$) as follows:

$$\frac{\partial c_T}{\partial t} = D_e \frac{\partial^2 c_T}{\partial x^2} - v_e \frac{\partial c_T}{\partial x} - \mu c_T \quad (25)$$

where R_T is the total retardation factor given by:

$$R_T = 1 + \frac{\rho k}{\theta} + \frac{a K_H}{\theta} \quad (26)$$

in which a is the air content, K_H is Henry's law constant accounting for linear equilibrium partitioning between the liquid and air phases, and D_e and v_e are the effective dispersion coefficient and pore-water velocity:

$$D_e = \frac{D}{R_T} \quad (27a)$$

$$v_e = \frac{v}{R_T} \quad (27b)$$

Jury et al. (1983) solved the transport model assuming that the chemical is uniformly incorporated at concentration C_i within the upper part ($0 \leq x \leq L$) of a semi-infinite profile (zero concentration below $x = L$) and subject to a third-

type boundary condition at the soil surface that accounts for volatilization into the air:

$$\left(-D_e \frac{\partial c_T}{\partial x} + v_e c_T \right)_{x=0} = -H_e C_T \quad (28)$$

where

$$H_e = \frac{D_a K_H}{d \theta R_T} \quad (29)$$

in which D_a is the gaseous diffusion coefficient. Equation 28 accounts for diffusion from the soil surface through a stagnant boundary layer of thickness d . The analytical solution of the above problem is (Jury et al., 1983):

$$c_T(x, t) = \frac{C_i}{2} \exp(-\mu t) \\ \times \left[\left[\operatorname{erfc} \left(\frac{x - L - v_e t}{2\sqrt{D_e t}} \right) - \operatorname{erfc} \left(\frac{x - v_e t}{2\sqrt{D_e t}} \right) \right] \right. \\ \left. + \left(1 + \frac{v_e}{H_e} \right) \exp \left(\frac{v_e x}{D_e} \right) \right. \\ \times \left[\operatorname{erfc} \left(\frac{x + L - v_e t}{2\sqrt{D_e t}} \right) - \operatorname{erfc} \left(\frac{x + v_e t}{2\sqrt{D_e t}} \right) \right] \\ + \left(2 + \frac{v_e}{H_e} \right) \exp \left(\frac{(H_e + v_e)(x + H_e t)}{D_e} - \mu t \right) \\ \times \left[\operatorname{erfc} \left(\frac{x + (2H_e + v_e)t}{2\sqrt{D_e t}} \right) \right. \\ \left. - \exp \left(\frac{H_e L}{D_e} \right) \operatorname{erfc} \left(\frac{x + L + (2H_e + v_e)t}{2\sqrt{D_e t}} \right) \right] \quad (30)$$

Here we give one example of the type of calculations that are typically carried out with SCREEN. The example is a slight modification of the TEST3 project that comes with the software. Various physical and solute transport parameters are entered in a window, as shown in figure 10, while figure 11 shows chemical parameter values, which can be selected from a database or provided upon input. The pa-

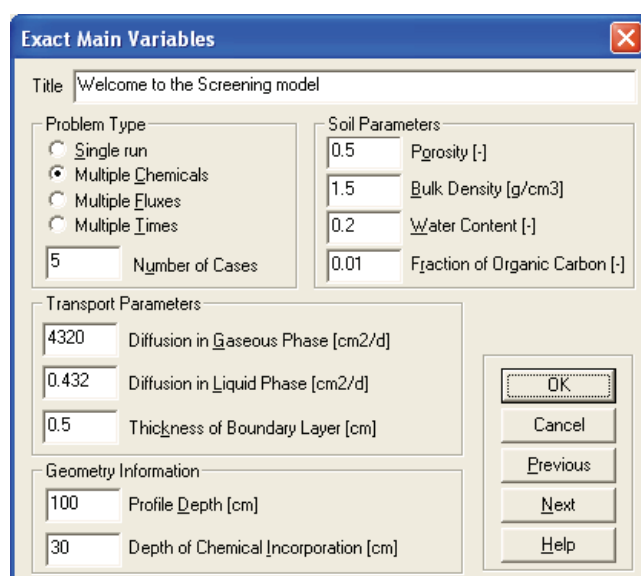


Figure 10. Window showing various input parameters needed for the screening model (SCREEN) of Jury et al. (1983).

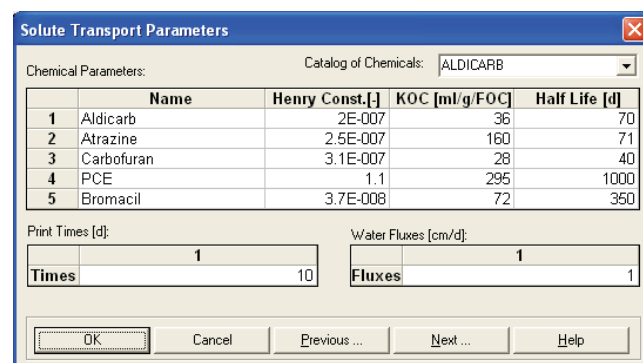


Figure 11. SCREEN window showing chemical and other parameters values used for the results shown in figure 11. The catalog of chemicals (upper right corner) can be used to select chemical parameters from a database included in the software.

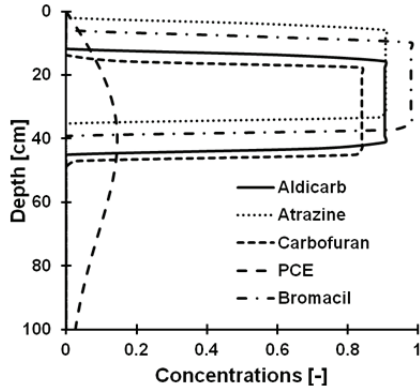


Figure 12. SCREEN window showing concentration distributions versus depth of several organic chemicals as obtained with the data shown in figures 11 and 12.

parameter K_{oc} in figure 11 is used to estimate the distribution coefficient (k) from the fraction of organic matter (f_{oc}) using $k = f_{oc}K_{oc}$.

Results of the transport model using the parameters from figures 10 and 11 are shown in figure 12. The example illustrates the interplay of sorption (more downward movement with lower K_{oc} values), degradation (lower maximum concentrations with increased degradation), and volatilization (lower total amount of mass in the profile and a more dispersed distribution, such as for PCE). Refer to articles by Jury et al. (1983, 1984a, 1984b) for detailed descriptions and several applications of their screening model.

THE 3DADE CODE

The 3DADE code (Leij and Bradford, 1994) may be used to evaluate analytical solutions for three-dimensional equilibrium solute transport in the subsurface. The solutions pertain to selected cases of three-dimensional transport during steady unidirectional water flow in porous media having uniform flow and transport properties. The transport equation contains terms to account for solute movement by advection and dispersion, as well as for solute retardation, first-order decay, and zero-order production. Like CXTFIT, the 3DADE code can be used to solve direct problems, in which concentrations are calculated as a function of time and space for specified model parameters, and for inverse problems, in which the program estimates selected parameters by fitting one of the analytical solutions to specified experimental data. Analytical solutions are provided in either Cartesian or cylindrical coordinate systems.

Figure 13 shows available simulation options that can be considered, in this case a rectangular source at the soil surface (or in groundwater perpendicular to the lateral flow direction). The governing transport equation for this example is given by:

$$R \frac{\partial c}{\partial t} = D_x \frac{\partial^2 c}{\partial x^2} - v \frac{\partial c}{\partial x} + D_y \frac{\partial^2 c}{\partial y^2} + D_z \frac{\partial^2 c}{\partial z^2} - \mu c + \gamma \quad (31)$$

with the initial and boundary conditions:

$$c(x, y, z) = C_i \quad (32)$$

$$(-D \frac{\partial c}{\partial x} + v c)|_{x=0+} = \begin{cases} vC_0 & |y| \leq a \quad |z| \leq b \\ 0 & |y| > a \quad |z| > b \end{cases} \quad (33)$$

$$\frac{\partial c}{\partial x}(\infty, y, z, t) = 0 \quad (34)$$

$$\frac{\partial c}{\partial y}(x, \pm\infty, z, t) = 0 \quad (35)$$

$$\frac{\partial c}{\partial z}(x, y, \pm\infty, t) = 0 \quad (36)$$

where x , y , and z are the three spatial coordinates, with flow occurring in the x direction; D_x is the longitudinal dispersion coefficient; D_y and D_z are transverse dispersion coefficients; and a and b define the lateral extent of the source at the inflow boundary. The analytical solution for this example is as follows (Leij et al., 1991):

$$\begin{aligned} c(x, y, z, t) = & \frac{\gamma}{\mu} \left(1 - e^{-\frac{\mu t}{R}} \right) \\ & + \frac{vC_0}{4\sqrt{\pi D_x R}} \int_0^t \frac{1}{\sqrt{\tau}} e^{-\frac{\mu \tau}{R}} \exp \left[-\frac{(Rx - v\tau)^2}{4DR\tau} \right] \\ & \times \left\{ \operatorname{erf} \left[\frac{(a+y)\sqrt{R}}{2\sqrt{D_y \tau}} \right] + \operatorname{erf} \left[\frac{(a-y)\sqrt{R}}{2\sqrt{D_y \tau}} \right] \right\} \\ & \times \left\{ \operatorname{erf} \left[\frac{(b+z)\sqrt{R}}{2\sqrt{D_z \tau}} \right] + \operatorname{erf} \left[\frac{(b-z)\sqrt{R}}{2\sqrt{D_z \tau}} \right] \right\} d\tau \\ & - \frac{v^2 C_0}{8D_x R \tau} \int_0^t \exp \left(\frac{vx}{D_x} \right) \operatorname{erfc} \left[\frac{Rx + v\tau}{2\sqrt{D_x R \tau}} \right] \\ & \times \left\{ \operatorname{erf} \left[\frac{(a+y)\sqrt{R}}{2\sqrt{D_y \tau}} \right] + \operatorname{erf} \left[\frac{(a-y)\sqrt{R}}{2\sqrt{D_y \tau}} \right] \right\} \\ & \times \left\{ \operatorname{erf} \left[\frac{(b+z)\sqrt{R}}{2\sqrt{D_z \tau}} \right] + \operatorname{erf} \left[\frac{(b-z)\sqrt{R}}{2\sqrt{D_z \tau}} \right] \right\} d\tau \\ & - \gamma \int_0^t e^{-\frac{\mu \tau}{R}} \left\{ \sqrt{\frac{v^2 \tau}{\pi D R^3}} \exp \left[\frac{(Rx - v\tau)^2}{4D_x R \tau} \right] \right. \\ & \left. + \frac{1}{2R} \operatorname{erfc} \left[\frac{Rx - v\tau}{2\sqrt{D_x R \tau}} \right] - \frac{1}{2R} \left(1 + \frac{vx}{D_x} + \frac{v^2 \tau}{D_x R} \right) \right\} (37) \\ & \times \exp \left(\frac{vx}{D_x} - \frac{\mu \tau}{R} \right) \operatorname{erfc} \left[\frac{Rx + v\tau}{2\sqrt{D_x R \tau}} \right] \left\} dt \end{aligned}$$

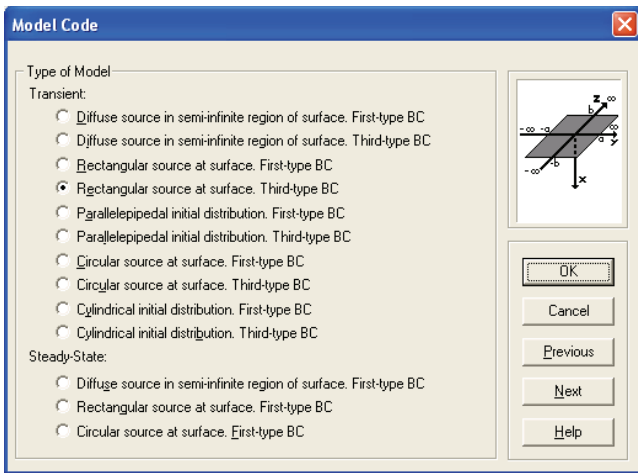


Figure 13. Available geometries, initial conditions, and inlet boundary conditions (BCs) that can be simulated using 3DADE within the STANMOD software package.

Figure 14 shows graphical output (x - y planar distributions for $z = 0$) obtained for this problem (EXAMPLE3 of 3DADE; figure 4 of Leij et al., 1991) assuming the following values for the geometry and input parameters: $v = 10 \text{ cm d}^{-1}$, $R = 1$, $\mu = \gamma = 0$, $D_x = 100 \text{ cm}^2 \text{ d}^{-1}$, $D_y = D_z = 10 \text{ cm}^2 \text{ d}^{-1}$, $C_o = 1 \text{ mg L}^{-1}$, $a = b = 7.5 \text{ cm}$, and $t = 1 \text{ d}$. Several other examples, including for circular coordinate systems, are discussed by Leij et al. (1991) and Leij and Bradford (1994).

THE N3DADE CODE

The N3DADE code of Leij and Toride (1997) is very similar to 3DADE, except that analytical solutions are

evaluated for three-dimensional nonequilibrium solute transport. Similar to 3DADE, N3DADE evaluates analytical solutions for three-dimensional transport during steady unidirectional water flow in macroscopically uniform porous media of semi-infinite length in the longitudinal direction, and of infinite length in the transverse directions. However, unlike 3DADE, only direct (forward) problems are considered in N3DADE.

As for the CFITIM and CXTFIT codes, nonequilibrium transport can be simulated in terms of physical (mobile-immobile or dual porosity) formulations, and chemical nonequilibrium assuming two sites (partial equilibrium, partial kinetic sorption). The formulations as such are extensions of the CFITIM and CXTFIT one-dimensional nonequilibrium transport equations to three dimensions. Refer to the article by Toride et al. (1993) and the N3DADE manual by Leij and Toride (1997) for detailed discussions of the governing transport equations, the analytical solutions, and several direct applications. Comprehensive sets of specific solutions are presented in these publications using Dirac, Heaviside, and exponential functions to describe a variety of initial, boundary, and production profiles. A rectangular or circular inflow area is specified for boundary value problems, while for initial and production value problems the respective initial and production profiles are defined for parallelepipedal, cylindrical, or spherical regions of the soil. Because of their complexity, these solutions are not restated here.

The N3DADE code within STANMOD comes with five preprogrammed examples, all taken from Leij and Toride (1997). They are for calculated concentration distributions, versus time or spatially, for instantaneous solute application

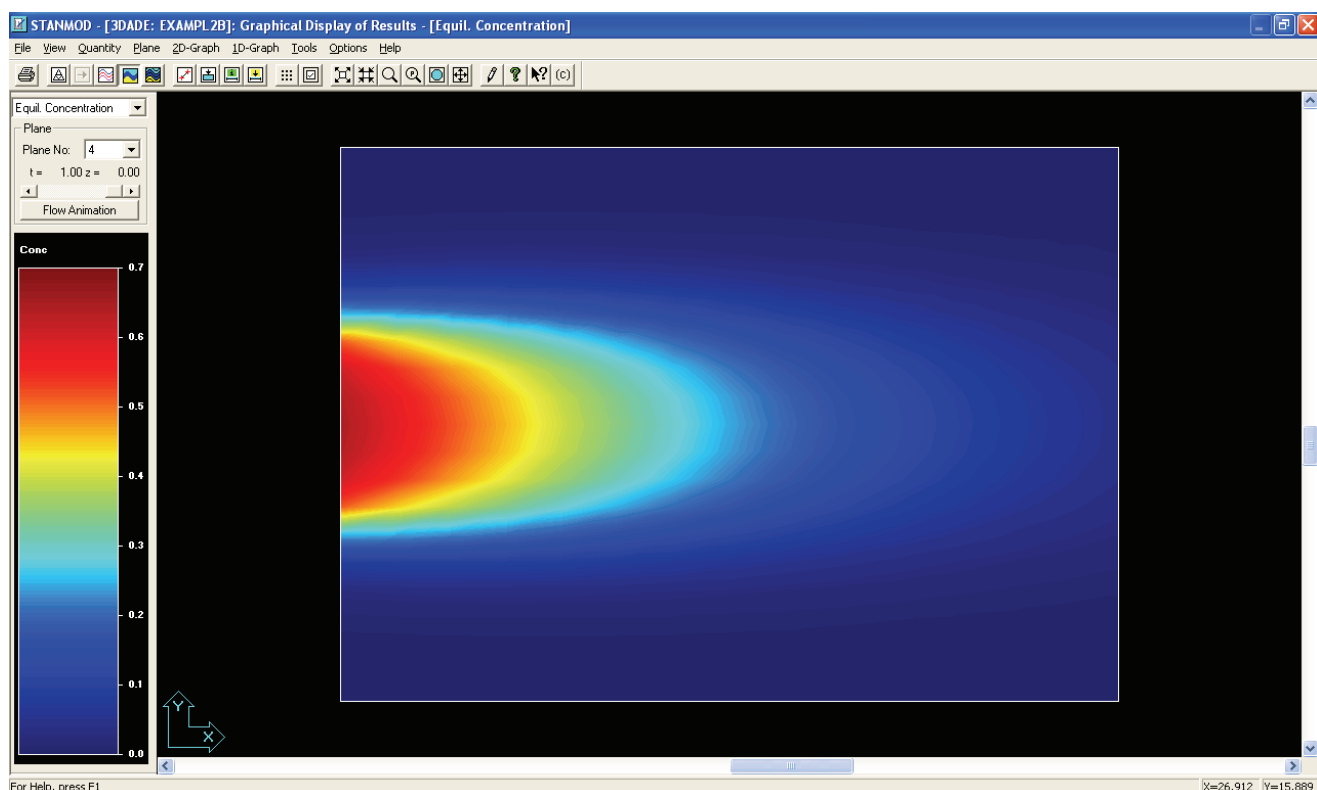


Figure 14. Graphical display of results obtained with STANMOD for the 3DADE example depicted in figure 13.

from a disk at the soil surface (a problem with circular geometry), solute application from a rectangular source at the soil surface (Cartesian geometry), and several initial and production value problems where the solute is initially located or produced within some finite circular or rectangular source within the transport domain. We further note two other applications of N3DADE to transport of a nonadsorbing dye (rhodamine) and cadmium in an alluvial aquifer by Pang and Close (1999a, 1999b).

FUTURE DEVELOPMENTS

Notwithstanding their limitations in terms of being restricted to linear problems (and hence homogeneous profiles, unidirectional flow that is constant in time and space, and the use of simplified initial and boundary conditions), analytical solutions likely will remain popular for a large number of applications. As shown also by many of the examples in this STANMOD overview, possible applications include initial or approximate analyses of subsurface transport, providing a better understanding of alternative transport processes and the effects of key transport parameters, predicting transport for large spatial or time scales, and estimating model parameters using inverse methods. The individual codes discussed in this review and included in STANMOD were developed for exactly those types of applications. The primary contribution of STANMOD is to include all of these codes in an easy-to-use, Windows-based framework for possible use by practitioners not necessarily familiar with the mathematical complexities of the separate programs. The GUIs of STANMOD are for this purpose very intuitive. They are used to manage the input data required to run STANMOD, as well as for editing, parameter allocation, problem execution, and visualization of results.

All computational programs were written in FORTRAN, and the graphical interfaces were written in MS Visual C++. The pre-processing unit includes specification of all necessary parameters to successfully run the FORTRAN codes. All post-processing is also carried out in the GUI. The post-processing unit consists of simple x-y plots for graphical presentation of the results (and data) and a dialog window that displays an ASCII output file. The multidimensional 3DADE and N3DADE codes are further supported with output graphics that include 2D contours (isolines or color spectra, as shown in this article) in real or cross-sectional views for equilibrium, nonequilibrium, and total concentrations. Output also includes animation of graphic displays at sequential time steps, and line graphs for selected boundary or internal sections, as well as for plots of variables versus time. Areas of interest can be zoomed into, and the vertical scale can be enlarged for cross-sectional views.

STANMOD is in public domain and can be downloaded freely (www.pc-progress.com/en/Default.aspx?stanmod). The software is supported by a discussion forum where users can submit questions or suggestions about the models. All projects included within STANMOD can also be downloaded separately from the website. While no definite plans

exist at present, new codes geared toward analytical models may be included in the future. In all, we believe that the different codes within STANMOD are serving an important role in the transfer of software technologies to both the scientific community and practitioners.

REFERENCES

- Antoniadis, V., and J. D. McKinley. 2003. Measuring heavy metal migration rates in low-permeable soil. *Environ. Chem. Lett.* 1(1):103-106.
- Bateman, H. 1910. The solution of a system of differential equations occurring in the theory of radioactive transformations. *Proc. Cambridge Phil. Soc.* 15: 423-427.
- Bauer P., S. Attinger, and W. Kinzelbach. 2001. Transport of a decay chain in homogenous porous media: Analytical solutions. *J. Contam. Hydrol.* 49(3-4): 217-239.
- Cho, C. M. 1971. Convective transport of ammonium with nitrification in soil. *Canadian J. Soil Sci.* 51(3): 339-350.
- Dagan, G. 1993. The Bresler-Dagan model of flow and transport: Recent theoretical developments. In *Water Flow and Solute Transport in Soils*, 13-32. D. Russo and G. Dagan, eds. Berlin, Germany: Springer-Verlag.
- Duke, C. L., R. C. Roback, P. W. Reimus, R. S. Bowman, T. L. McLing, K. E. Baker, and L. C. Hull. 2007. Elucidation of flow and transport processes in a variably saturated system of interlayered sediment and fractured rock using tracer tests. *Vadose Zone J.* 6(4): 855-867.
- Gamerding, A. P., R. J. Wagenet, and M. Th. van Genuchten. 1990. Application of two-site/two-region models for studying simultaneous nonequilibrium transport and degradation of pesticides. *SSSA J.* 54(4): 957-963.
- Gaur, A., R. Horton, D. B. Jaynes, J. Lee, and S. A. Al-Jabri. 2003. Using surface time domain reflectometry measurements to estimate subsurface chemical movement. *Vadose Zone J.* 2(4): 539- 543.
- Higashi, K., and T. H. Pigford. 1980. Analytical models for migration of radionuclides in geologic sorbing media. *J. Nucl. Sci. Tech.* 17(9): 700-709.
- Huang, K., N. Toride, and M. Th. van Genuchten. 1995. Experimental investigation of solute transport in large, homogeneous and heterogeneous, saturated soil columns. *Transport in Porous Media* 18(3): 283-302.
- Jacobsen, O. H., F. J. Leij, and M. Th. van Genuchten. 1992a. Parameter determination for chloride and tritium transport in undisturbed lysimeters during steady flow. *Nordic Hydrol.* 23(2): 89-104.
- Jacobsen, O. H., F. J. Leij, and M. Th. van Genuchten. 1992b. Lysimeter study of anion transport during steady flow through layered coarse-textured soil profiles. *Soil Sci.* 154(3): 196-205.
- Javandel, I., C. Doughty, and Chin-Fu Tsang. 1984. *Groundwater Transport: Handbook of Mathematical Models*. Water Resources Monograph No. 10. Washington, D.C.: American Geophysical Union.
- Jensen, K. H., G. Destouni, and M. Sassner. 1996. Advection-dispersion analysis of solute transport in undisturbed soil monoliths. *Ground Water* 34(6): 1090-1097.
- Jury, W. A., L. H. Stolzy, and P. Shouse. 1982. A field test of the transfer function model for predicting solute transport. *Water Resour. Res.* 18(2): 369-375.
- Jury, W. A., W. F. Spencer, and W. J. Farmer. 1983. Behavior assessment model for trace organics in soil: I. Description of model. *J. Environ. Qual.* 12(4):558-564.
- Jury, W. A., W. J. Farmer, and W. F. Spencer. 1984a. Behavior assessment model for trace organics in soil: II. Chemical

- classification and parameter sensitivity. *J. Environ. Qual.* 13(4): 4: 567-572.
- Jury, W. A., W. F. Spencer, and W. J. Farmer. 1984b. Behavior assessment model for trace organics in soil: IV. Review of experimental evidence. *J. Environ. Qual.* 13(4): 580-586.
- Kamra, S. K., B. Lennartz, M. Th. van Genuchten, and P. Widmoser. 2001. Evaluating non-equilibrium solute transport in small columns. *J. Contam. Hydrol.* 48(3-4): 189-212.
- Kasteel, R., T. Pütz, J. Vanderborght, and H. Vereecken. 2010. Fate of two herbicides in zero-tension lysimeters and in field soil. *J. Environ. Qual.* 39(4): 1451-1466.
- Kay, J. T., and M. H. Conklin. 2001. Processes of nickel and cobalt uptake by a manganese oxide forming sediment in Pinal Creek, Globe mining district, Arizona. *Environ. Sci. Tech.* 35(24): 4719-4725.
- Koestel, J. K., J. Moeyns, and N. J. Jarvis. 2011. Evaluation of nonparametric shape measures for solute breakthrough curves. *Vadose Zone J.* 10(4): 1261-1275.
- Köhne, J. M., S. Schlüter, and H.-J. Vogel. 2011. Predicting solute transport in structured soil using pore network models. *Vadose Zone J.* 10(3): 1082-1096.
- Konikow, L. F., and J. D. Bredehoeft. 1992. Ground-water models cannot be validated. *Advances in Water Resources* 15(1): 75-83.
- Lapidus, L., and N. R. Amundson. 1952. Mathematics of adsorption in beds: VI. The effect of longitudinal diffusion in ion exchange chromatographic columns. *J. Phys. Chem.* 56(8): 984-988.
- Leij, F. J., and S. A. Bradford. 1994. 3DADE: A computer program for evaluating three-dimensional equilibrium solute transport in porous media. Research Report No. 134. Riverside, Cal.: USDA-ARS U.S. Salinity Laboratory.
- Leij, F. J., and N. Toride. 1997. N3DADE: A computer program for evaluating nonequilibrium three-dimensional equilibrium solute transport in porous media. Research Report No. 143. Riverside, Cal.: USDA-ARS U.S. Salinity Laboratory.
- Leij, F. J., and N. Toride. 1998. Chapter 5: Analytical solutions for nonequilibrium transport models. In *Physical Nonequilibrium in Soils: Modeling and Application*, 117-156. H. M. Selim and L. Ma, eds. Chelsea, Mich.: Ann Arbor Press.
- Leij, F. J., T. H. Skaggs, and M. Th. van Genuchten. 1991. Analytical solutions for solute transport in three-dimensional semi-infinite porous media. *Water Resour. Res.* 27(10): 2719-2733.
- Lindstrom, F. T., R. Haque, V. H. Freed, and L. Boersma. 1967. The movement of some herbicides in soils: Linear diffusion and convection of chemicals in soils. *Environ. Sci. Tech.* 1(7): 561-565.
- Marquardt, D. W. 1963. An algorithm for least-squares estimation of nonlinear parameters. *SIAM J. Appl. Math.* 11(2): 431-441.
- Mayer, A., T. Sandman, and M. Breidenbach. 2008. Effect of flow regime on physical nonequilibrium transport in unsaturated porous media. *Vadose Zone J.* 7(3): 981-991.
- Oreskes, N., K. Shrader-Frechette, and K. Belitz. 1994. Verification, validation, and confirmation of numerical models in the earth sciences. *Science* 263(5147): 641-646.
- Pace, M. N., M. A. Mayes, P. M. Jardine, T. L. Mehlhorn, J. M. Zachara, and B. N. Bjornstad. 2003. Quantifying the effects of small-scale heterogeneities on flow and transport in undisturbed cores from the Hanford formation. *Vadose Zone J.* 2(4): 664-676.
- Pang, L., and M. Close. 1999a. Field-scale physical nonequilibrium transport in an alluvia aquifer. *J. Contam. Hydrol.* 38(4): 447-464.
- Pang, L., and M. Close. 1999b. A field study of nonequilibrium and facilitated transport of Cd in an alluvial gravel aquifer. *Ground Water* 37(5): 785-792.
- Parker, J. C., and M. Th. van Genuchten. 1984. Determining transport parameters from laboratory and field tracer experiments. Bulletin 84-3. Blacksburg, Va.: Virginia Agricultural Experiment Station.
- Pérez Guerrero, J. S., L. C. G. Pimentel, T. H. Skaggs, and M. Th. van Genuchten. 2009. Analytical solution of the advection-diffusion transport equation using a change-of-variable and integral transform technique. *Intl. J. Heat and Mass Transfer* 52(13-14): 3297-3304.
- Pérez-Guerrero, J. S., T. H. Skaggs, and M. Th. van Genuchten. 2010. Analytical solution for multi-species contaminant transport subject to sequential first-order decay reactions in finite media. *Transport in Porous Media* 80(2): 373-387.
- Pivetz, B. E., and T. S. Steenhuis. 1995. Soil matrix and macropore biodegradation of 2,4-D. *J. Environ. Qual.* 24(4): 564-570.
- Pontedeiro, E. M., P. F. L. Heilbron, and R. M. Cotta. 2007. Assessment of the mineral industry NORM/TENORM disposal in hazardous landfills. *J. Hazard. Materials* 139(3): 563-568.
- Šejna, M., J. Šimůnek, and M. Th. van Genuchten. 2011. The HYDRUS software package for simulating two- and three-dimensional movement of water, heat, and multiple solutes in variably saturated media. User Manual, Version 2.0. Prague, Czech Republic: PC Progress.
- Seuntjens, P., K. Tirez, J. Šimůnek, M. Th. van Genuchten, C. Cornelis, and P. Geuzens. 2001. Aging effects on cadmium transport in undisturbed contaminated sandy soil columns. *J. Environ. Qual.* 30(3): 1040-1050.
- Šimůnek, J., and J. W. Hopmans. 2002. Chapter 1.7: Parameter optimization and nonlinear fitting. In *Methods of Soil Analysis: Part 1. Physical Methods*, 139-157. J. H. Dane and G. C. Topp, eds. Madison, Wisc.: SSSA.
- Šimůnek, J., M. Th. van Genuchten, M. Šejna, N. Toride, and F. J. Leij. 1999. The STANMOD computer software for evaluating solute transport in porous media using analytical solutions of convection-dispersion equation. Versions 1.0 and 2.0. IGWMC-TPS-71. Golden, Colo.: Colorado School of Mines, International Ground Water Modeling Center.
- Šimůnek, J., M. Th. van Genuchten, and M. Šejna. 2008a. Development and applications of the HYDRUS and STANMOD software packages and related codes. *Vadose Zone J.* 7(2): 587-600.
- Šimůnek, J., M. Šejna, H. Saito, M. Sakai, and M. Th. van Genuchten. 2008b. The HYDRUS-1D software package for simulating the movement of water, heat, and multiple solutes in variably saturated media. Version 4.0. HYDRUS Software Series 3. Riverside, Cal.: University of California, Department of Environmental Sciences.
- Šimůnek, J., M. Th. van Genuchten, and M. Šejna. 2012. HYDRUS: Model use, calibration, and validation. *Trans. ASABE* 55(4): 1263-1276.
- Skaggs, T. H., and F. J. Leij. 2002. Chapter 6.3: Solute transport: Theoretical background. In *Methods of Soil Analysis: Part 4. Physical Methods*, 1353-1380. J. H. Dane and C.G. Topp, eds. Madison, Wisc.: SSSA.
- Spurlock, F. C., K. Huang, and M. Th. van Genuchten. 1995. Isotherm nonlinearity and nonequilibrium sorption effects on transport of fenuron and monuron in soil columns. *Environ. Sci. Tech.* 29(4): 1000-1007.
- Srinivasan, V., and T. P. Clement. 2008. Analytical solutions for sequentially coupled one-dimensional reactive transport problems: Part II. Special cases, implementation, and testing. *Adv. Water Resour.* 31(2): 219-232.
- Srivastava, P., S. M. Sanders, J. H. Dane, Y. Feng, J. Basile, and

- M. O. Barnett. 2009. Fate and transport of sulfadimethoxine and ormetoprim in two southeastern United States soils. *Vadose Zone J.* 8(1): 32-41.
- Tao, Y. Q., Y. R. Bian, X. L. Yang, and F. Wang. 2009. Transport of malathion in homogeneous soil liquid chromatographic columns: Influence of nonequilibrium sorption. *Vadose Zone J.* 8(1): 42-51.
- Tilahun, K., J. F. Botha, and A. T. P. Bennie. 2005. Transport of bromide in the Bainsvlei soil: Field experiment and deterministic/stochastic model simulation. II. Intermittent water application. *Soil Res.* 43(1): 81-85.
- Toride, N., and F. J. Leij. 1996a. Convective dispersive stream tube model for field-scale solute transport: I. Moment analysis. *SSSA J.* 60(2): 342-352.
- Toride, N., and F. J. Leij. 1996b. Convective dispersive stream tube model for field-scale solute transport: II. Examples and calibration. *SSSA J.* 60(2): 352-361.
- Toride, N., F. J. Leij, and M. Th. van Genuchten. 1993. A comprehensive set of analytical solutions for nonequilibrium solute transport with first-order decay and zero-order production. *Water Resour. Res.* 29(7): 2167-2182.
- Toride, N., F. J. Leij, and M. Th. van Genuchten. 1999. The CXTFIT code for estimating transport parameters from laboratory or field tracer experiments. Version 2.1. Research Report No. 137. Riverside, Cal.: USDA-ARS U.S. Salinity Laboratory.
- Toride, N., M. Inoue, and F. J. Leij. 2003. Hydrodynamic dispersion in an unsaturated dune sand. *SSSA J.* 67(3): 703-712.
- Vanderborght, J., R. Kasteel, M. Herbst, M. Javaux, D. Thiéry, M. Vanclooster, C. Mouvet, and H. Vereecken. 2005. A set of analytical benchmarks to test numerical models of flow and transport in soils. *Vadose Zone J.* 4(1): 206-221.
- Vanderborght, J., R. Kasteel, and H. Vereecken. 2006. Stochastic continuum transport equations for field-scale solute transport: Overview of theoretical and experimental results. *Vadose Zone J.* 5(1): 184-203.
- van Genuchten, M. Th. 1974. Mass transfer studies in sorbing porous media. PhD diss. Las Cruces, N.M.: New Mexico State University.
- van Genuchten, M. Th. 1980. Determining transport parameters from solute displacement experiments. Research Report No. 118. Riverside, Cal.: USDA-ARS U.S. Salinity Laboratory.
- van Genuchten, M. Th. 1981a. Non-equilibrium transport parameters from miscible displacement experiments, Research Report No. 119. Riverside, Cal.: USDA-ARS U.S. Salinity Laboratory.
- van Genuchten, M. Th. 1981b. Analytical solutions for chemical transport with simultaneous adsorption, zero-order production, and first-order decay. *J. Hydrol.* 49(3-4): 213-233.
- van Genuchten, M. Th. 1985. Convective-dispersive transport of solutes involved in sequential first-order decay reactions. *Computers and Geosci.* 11(2): 129-147.
- van Genuchten, M. Th., and W. J. Alves. 1982. Analytical solutions of the one-dimensional convective-dispersive solute transport equation. Tech. Bulletin 1661. Washington, D.C.: USDA-ARS.
- van Genuchten, M. Th., and R. W. Cleary. 1979. Movement of solutes in soils: Computer-simulated and laboratory results. In *Soil Chemistry: B. Physico-Chemical Models*, 349-386. G. H. Bolt, ed. Developments in Soil Science 5B. Amsterdam, The Netherlands: Elsevier Scientific.
- van Genuchten, M. Th., and J. C. Parker. 1984. Boundary conditions for displacement experiments through short laboratory soil columns. *SSSA J.* 48(4): 703-708.
- van Genuchten, M. Th., and P. J. Wierenga. 1976. Mass transfer studies in sorbing porous media: I. Analytical solutions. *SSSA J.* 40(4): 473-480.
- Wellman, D. M., J. M. Zachara, C. Liu, N. P. Qafoku, S. C. Smith, and S. W. Forrester. 2008. Advective desorption of uranium(IV) from contaminated Hanford vadose zone sediments under saturated and unsaturated conditions. *Vadose Zone J.* 7(4): 1144-1159.
- Wernberg, T. 1998. Multicomponent groundwater transport with chemical equilibrium and kinetics: Model development and evaluation. *Hydrol. Sci. J.* 43(2): 299-317.